Chem. Senses 39: 617–629, 2014
doi:10.1093/chemse/bju035
Advance Access publication July 23, 2014

Transplanted Human Adipose Tissue-Derived Stem Cells Engraft and Induce Regeneration in Mice Olfactory Neuroepithelium in Response to Dichlobenil Subministration

Valeria Franceschini[1], Simone Bettini[1], Simone Pifferi[2], Anna Menini[2], Gabriele Siciliano[3], Emanuela Ognio[4], Anna Teresa Brini[5], Enrico Di Oto[6] and Roberto P. Revoltella[7]

[1]Department of Biological, Geological and Environmental Sciences, University of Bologna, and Foundation Onlus Stem Cells and Life, Via Selmi 3, 40126 Bologna, Italy, [2]International School for Advanced Studies, SISSA, Via Bonomea 265, 34136 Trieste, Italy, [3]Department of Clinical and Experimental Medicine, University of Pisa, Via Roma 67, 56126 Pisa, Italy, [4]IRCCS San Martino, National Institute for Cancer Research (IST), Largo Rosanna Benzi 10, 16132 Genua, Italy, [5]Department of Biomedical, Surgical and Odontoiatric Sciences, University of Milan, Via Vanvitelli 32, 2019 Milan, Italy, [6]Department of Hematology and Oncology "L. and A. Seragnoli," Section of Anatomic Pathology at Bellaria Hospital, University of Bologna, Via Altura 3, 40139 Bologna, Italy and [7]Institute for Chemical, Physical Processes, C.N.R. and Foundation Onlus Stem Cells and Life, Via L.L. Zamenhof 8, 56127 Pisa, Italy

Correspondence to be sent to: Valeria Franceschini, Department of Biological, Geological and Environmental Sciences, University of Bologna, Via Selmi 3, 40126 Bologna, Italy. e-mail: *valeria.franceschini@unibo.it*

Accepted June 2, 2014

Abstract

We used immunodeficient mice, whose dorsomedial olfactory region was permanently damaged by dichlobenil inoculation, to test the neuroregenerative properties of transplanted human adipose tissue-derived stem cells after 30 and 60 days. Analysis of polymerase chain reaction bands revealed that stem cells preferentially engrafted in the lesioned olfactory epithelium compared with undamaged mucosa of untreated transplanted mice. Although basal cell proliferation in untransplanted lesioned mice did not give rise to neuronal cells in the olfactory mucosa, we observed clusters of differentiating olfactory cells in transplanted mice. After 30 days, and even more at 60 days, epithelial thickness was partially recovered to normal values, as also the immunohistochemical properties. Functional reactivity to odorant stimulation was also confirmed through electro-olfactogram recording in the dorsomedial epithelium. Furthermore, we demonstrated that engrafted stem cells fused with mouse cells in the olfactory organ, even if heterokaryons detected were too rare to hypothesize they directly repopulated the lesioned epithelium. The data reported prove that the migrating transplanted stem cells were able to induce a neuroregenerative process in a specific lesioned sensory area, enforcing the perspective that they could become an available tool for stem cell therapy.

Key words: herbicide, *Nod-scid* mice, olfactory mucosa, stem cell transplantation, tissue recovery

Introduction

Olfaction is essential to most animals, in order to mediate numerous behavioral repertoires such as food search, intra- and inter-specific interactions, and reproduction (Zarzo 2007). Accordingly, they are equipped with a complex olfactory system based on highly specialized chemosensory cells, the olfactory sensory neurons (OSNs) embedded in the olfactory epithelium (OE). In vertebrates the OE, lining the posterior half of the nasal cavity, the nasal septum, and, in mammals, also the bony turbinates, is in direct contact with the environment, as it must be to detect and transduce odorous compounds (Farbman 1990; Mori and Yoshihara 1995).

Because of their relatively unprotected position, the OSNs can be easily damaged by physical injury, by exposure to

inhaled environmental pollutants and viruses, and are a known-entry route into the brain for pathogens and chemicals (Shipley 1985; Lewis and Dahl 1995; Tjälve et al. 1996; Mori et al. 2002;Vent et al. 2003, 2004; Jacquot et al. 2006). As a consequence of this vulnerability, the OSNs are continuously replaced throughout life by new elements originating from progenitors in the basal layer. Several classes of chemicals are known to induce OE histopathological changes, particularly organic solvents (Cruzan et al. 2002; Kasai et al. 2002; Buron et al. 2009), heavy metals (Bettini et al. 2006; Keller et al. 2006), and herbicides (Bergman et al. 2002; Kim et al. 2010). The proliferation of basal stem cells and their differentiation to neurons establishing new bulbar connections can completely recover histological and functional integrity in a wide range of lesions induced by toxicants (Schwob et al. 1995; Weruaga et al. 2000; Bergman et al. 2002). The time course of regeneration was measured: OE was completely restored within 6–8 weeks after methyl bromide-induced damage (Schwob et al. 1995), while reinnervation by 8 weeks (Schwob et al. 1999), even if receptotopy is not fully preserved. In some cases, chemical exposure can lead to chronic damage. Dichlobenil (DCB) is a commonly used herbicide, which, when intraperitoneally injected, induces extensive necrosis in mice dorsomedial OE, with permanent effects (Bergman et al. 2002; Franceschini et al. 2009a, 2009b). The damaged region shows a respiratory epithelial metaplasia with invaginations into a fibrotic *lamina propria*, almost completely devoid of Bowman's glands, a possible cause of the irreversible damage. As a consequence of these toxic properties, DCB is suitable for creating an hyposmic animal model lacking neuronal stem cells in the dorsomedial olfactory region.

In recent years, stem cell transplantation has received considerable attention owing to its potential application in neurological disorder therapies. Different stem cell types, from various sources, have been studied for their effectiveness in neural replacement strategies, including: embryonic stem cells; neural stem cells from fetal or adult brain regions, in particular those from the sub-ventricular zone or dentate gyrus of the hippocampus; induced pluripotent stem cells; and a range of non-neural stem cells comprising of mesenchimal stem cells (MSCs) (Kim and de Vellis 2009; Gögel et al. 2011). Although bone marrow has for years represented the main source of MSCs in research and therapeutic studies, multipotent stem cells from more accessible sources, such as adipose tissue, have attracted great interest because of their advantages. Adipose derived stem cells (ADSCs) express the same surface markers of MSCs (Zuk et al. 2002; Lee et al. 2004), but their cell proliferation rate is higher than that of bone marrow-derived MSCs (Lee et al. 2004). Moreover, they can be isolated by a less invasive method and in larger quantities compared with bone marrow-derived MSCs. In culture, they have shown an impressive developmental plasticity, undergoing adipogenic, myogenic, chondrogenic, and osteogenic differentiation when treated with lineage-specific factors (Lee et al. 2004; Chen et al. 2012). Following neural induction ADSCs displayed immunocytochemical staining for neural stem cell markers (nestin), neuronal markers (NeuN), astrocyte markers (GFAP), and oligodendrocyte markers (CNPase) in vitro (Safford et al. 2002; Dhar et al. 2007; Jang et al. 2010). Furthermore, ADSCs could be converted into neurospheres able to differentiate into functionally active Schwann cell-like cells forming myelin structures with neuronal neurites in vitro (Xu et al. 2008). When the cells are engrafted in rats with surgically injured spinal cord, they are able to form a myelin sheath on Central Nervous System axons (Chi et al. 2010). Several recent studies also confirmed ADSCs capacity to enhance peripheral nerve regeneration and functional recovery in sciatic nerve defects (Liu et al. 2011, Scholz et al. 2011; Gu et al. 2012). Moreover, transplantation of ADSCs in rat with intracerebral hemorrhage promoted neuronal differentiation of implanted cells, tissue protection from apoptosis, and improvement of neurological function (Chen et al. 2012).

In a previous research (Franceschini et al. 2009a, 2009b), we observed that hematopoietic stem cells (UCB-CD133^{+}), transplanted in *nod-scid* mice subjected to DCB inoculation, gave rise to an early regenerative process of the olfactory organ after 31 days. In the present study, we intended to evaluate the engraftment efficiency and the therapeutic potential of ADSCs in restoring olfactory integrity in acute lesioned mice.

Materials and methods

Animals

We used immunodeficient *Nod-scid* mice as xenotransplantation model to prevent immune rejection. Mice were purchased from Charles River Laboratories, maintained in sterile Micro-Isolator cages, and given ad libitum access to autoclaved food and acidified water, to prevent bacterial growth.

Stem cell isolation

ADSCs were obtained from aspirated subcutaneous adipose tissues from 8 female donors (aged 28–42 years) under informed consent. Fresh lipoaspirates were washed in phosphate-buffered saline (PBS), then minced, transferred to Dulbecco's modified Eagle medium (DMEM) supplemented with penicillin (50 µg/mL), streptomycin (50 µg/mL), and 2 mM l-glutamine (control medium, CM) and digested using collagenase at 37°C for 30 min. Fragments were centrifuged (300 × *g* for 3 min), neutralized in CM containing 10% FCS (CM-FCS), and centrifuged again to complete the separation of the ADSCs-rich pellet from the primary adipocytes. The cells were cultured for at least 4 weeks, changing CM-FCS twice a week. From 2 mL of lipoaspirate, approximately 1×10^6 cells were usually generated. Adherent cells proliferated

with an average doubling time of approximately 65 h, without significant difference in growth rate between cells derived from different lipoaspirates. Their clonogenic potential, tested by the CFU-F assay (the cells were cultured for 14 days, methanol fixed, stained with Giemsa and clusters >50 cells counted), was variable with an average of 5 CFU-F for 1×10^6 seeded cells (from a minimum of 4% to a maximum of 12%). At the second passage, the cell population showed a homogeneous fibroblast-like shape. Their phenotypic profile was tested by cytofluorometric analysis (FASCalibur System, Becton-Dickinson). In excess of 90%, the ADSCs at the fourth cell passage expressed CD44, CD73, CD105, CD90, and HLA-ABC, whereas there was less than 2% positive for CD14 and HLA.DPQR, and cells did not express CD45, CD71, and CD106, confirming the ADSCs marker expression reported in literature (Lee et al. 2004; de Girolamo et al. 2007).

Transplantation

This study was approved by the ethics committee (Ethic Committee of the Institute for Research against Tumors [IST] of Genua and Ethic Committee of the Italian National Research Council CNR]), and all experimental procedures were carried out in accordance with their guidelines. Thirty-six 2-month-old female inbred *nod-scid* mice were used (Figure 1). Twenty-four mice were injected i.p. twice (to minimize side effects) with DCB (Fluka) dissolved in DMSO (1 mL/g) (Bergman et al. 2002) on days 0 (50 mg/kg body weight) and 7 (20 mg/kg). Then, on day 2, each mouse was sublethally irradiated with a dose of 3.5 Gy, commonly used in transplantation protocols and sensibly less than the lethal dose of 7.5 Gy (Diaz et al. 2012b). This is a necessary recipient conditioning to enhance engraftment of transplanted human MSCs in several tissues other than their primary residence sites (Mouiseddine et al. 2007), as irradiation induces an increased concentration of chemoattractants, especially in injured tissues (see also Tabatabai et al. 2006). On day 9, 16 mice (Group A) were transplanted with previously isolated human ADSCs (75 000–100 000 viable cells from 1 donor per mouse) by tail vein injection, whereas the other 8 DCB-treated mice (Group B) were used as controls and injected with saline alone. The remaining 12 animals not injected with the herbicide were divided into 2 groups: 4 mice (Group C) were treated with vehicles only (DMSO and saline) and 8 mice (Group D) were transplanted with ADSCs, analogously to Group A, after sublethal irradiation. Some of the mice were used for electrophysiological recording prior to sacrifice.

Tissue sampling

Thirty and 60 days later, 8 mice from Group A, 4 mice from Group B, 2 mice from Group C, and 4 mice from Group D were sacrificed using carbon dioxide asphyxiation, on each occasion. They were dissected and different organs and tissues were collected for various assays: kidney, skin, and liver were

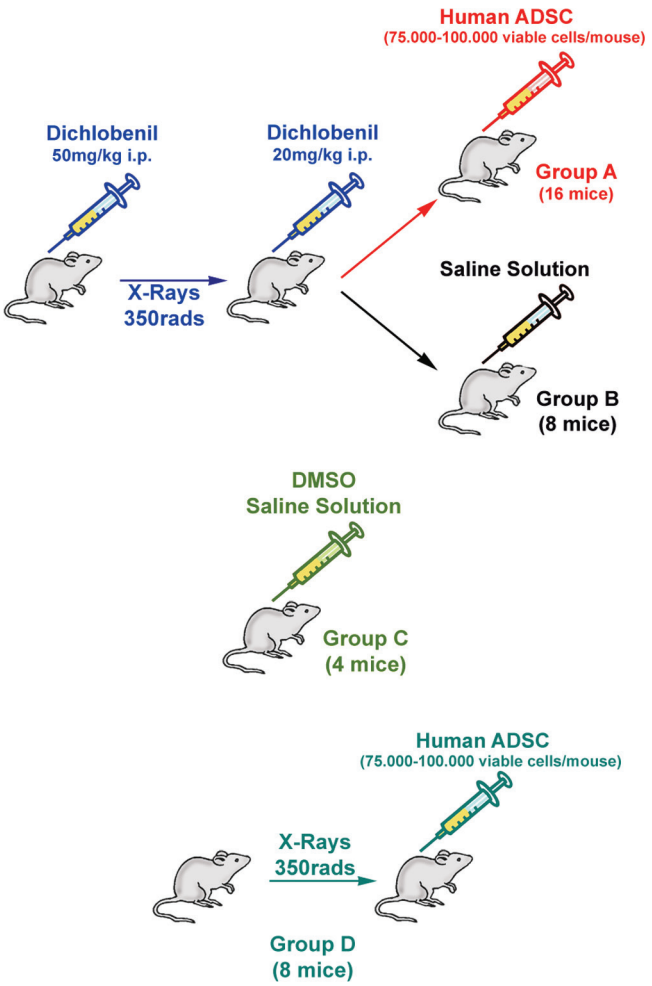

Figure 1 Experimental model. Day 0, 24 *nod/scid* mice were injected with DCB (50 mg/kg); day 2 they were sublethally irradiated, and day 7 injected again with DCB (20 mg/kg). Two days later, 16 mice were transplanted with ADSCs by tail vein injection (Group A) and 8 mice (Group B) with saline alone and used as controls. Four mice (Group C) were treated with the vehicle alone (DMSO, 1 mL/g) on days 0 and 7 and injected with saline solution on day 9. The remaining 8 mice (Group D) were irradiated and transplanted with ADSCs.

immediately chilled in ice, frozen in liquid nitrogen, and then kept at −24°C for DNA analysis; the nasal region was divided into left and right halves: one was fixed by immersion in modified Bouin's fluid, made up of a saturated aqueous solution of picric acid and formalin (ratio 3:1), for 24 h, paraffin embedded, sectioned (5 µm) and subjected to immunohistochemical, lectin staining and fluorescence in situ hybridization procedures (see Franceschini et al. 2009a for details), whereas the other was processed with kidney, skin, and liver.

DNA analysis

Polymerase chain reaction (PCR) assays were performed on total genomic DNA extracts (for details, see Franceschini et al. 2009a) to evaluate the engraftment of donor cells in all tissue samples by means of the

presence of the human-DNA HLA-DQα1 sequence. We used (5-GTGCTGCAGGTGTAAACTTGTACCAGTT GT-3) and (5-CACGGATCCGGTAGCAGCGGTAGAAG TTG-3) as the forward and reverse primers, respectively. To establish the sensitivity of our PCR assays for human DNA in murine DNA samples, we adopted the method of amplification employing Taq platinum using as reference standard curves for decreasing amounts of human ADSC DNA (from 1000 ng to 1 pg) in normal mouse liver DNA, up to 1 mg of total DNA sample in 10 mL. This method detects 1 ng of human DNA in 1 mg mouse DNA, after 40 cycles. To exclude potential contaminations, randomly chosen samples positive for HLA-DQα1 (Group A mice no. 3, 6, 10, and 14) were additionally analyzed for the presence of 3 human-specific STRs (D8S1179, D18S51, and D21S11) selected from the Combined DNA Index System (CODIS), commonly used for paternity testing and other forensic applications.

Immunohistochemistry

Antibodies used in this study were 1) mouse monoclonal Ab to GAP-43 (1:500; Clone GAP-7B10; Sigma), a phosphoprotein known to be expressed during axonal growth; 2) rabbit polyclonal Ab to Olfactory Marker Protein (OMP) (1:500; Santa Cruz Biotechnology), expressed in fully differentiated OSNs; 3) mouse monoclonal Ab to PCNA (1:500; Clone PC10; Sigma) a nucleoplasmic protein most abundant during S-phase of the cell cycle; 4) rabbit polyclonal Ab to PGP 9.5 (1:300; DAKO Cytomation), a marker expressed by mature and immature OSNs and vomeronasal neurons; 5) rabbit polyclonal Ab to neurotrophic tyrosine kinase receptor type B (TrkB) (1:100; Santa Cruz Biotechnology), expressed by immature OSNs. Sections were processed according to the manufacturer's protocols; in brief, they were deparaffinized, rehydrated, incubated with 3% hydrogen peroxide to quench endogenous peroxidase activity, and then heated by microwave in citrate buffer pH 6.0 for antigen retrieval, for 10 min at 750 W. After blocking with 10% normal goat serum (NGS; Vector Laboratories), the sections were incubated separately overnight at 4°C with primary antibodies. The sections were then washed and incubated for 1 h and 30 min in peroxidase-labeled goat anti-rabbit (1:100; Vector Laboratories) or mouse (1:100; Sigma) IgG. The immunoreaction was visualized by treating the sections with 3,3 diaminobenzidine (DAB; Sigma). The sections, except those treated with anti-PCNA, were then counterstained with Gill's Hematoxylin (Sigma), dehydrated, and coverslipped with Permount (Fisher Scientific). Negative controls were provided by omission of the primary antibody, which was replaced by 3% NGS. All the controls were negative.

Lectin histochemistry

In this procedure, the lectin used was *Bandeirea simplicifolia* agglutinin isolectin B_4 (BSA-I-B_4) (10 µg/mL; Carbohydrate specificity: α-galactose; Inhibitory agent: Gal (200 mM); Sigma Chemical). Lectin histochemistry was performed as follows: after dewaxing, rehydration and peroxidase block, the slides were incubated for 3 h with lectin (10 µg/mL in TBS 0.1 M) at room temperature in a moist chamber. The sections were then processed as described for immunohistochemistry. Negative controls included competitive inhibition with the appropriate sugar (100–200 mM) for 1 h at room temperature and buffered saline instead of the lectin.

Image analysis

Morphometric and densitometric analysis was performed on 2 adjacent sequences (for PCNA and OMP quantification) of semi-serial sections at 0.2 mm intervals using the Image J software (v. 1.41o). We used 8 mice from Group A at 30 days, 8 from Group A at 60 days, 4 from Group B, 4 from Group D, and 4 from Group C.

Dorsomedial OE thickness was measured from basal lamina to apical surface, excluding cilia length, averaging 3 measurements for each section. The mean values of all sections represent the epithelial depth for every specimen (we used all mice of each group).

For evaluation of proliferative activity in the dorsal OE, all PCNA-positive nuclei were counted in the semi-serial sections, the data collected from each olfactory organ were averaged and expressed as number of $PCNA^+$ cells per unit length, accordingly to Monticello et al. (1990).

To estimate the amount of mature OSNs, we chose optical density (OD) rather than cell counts because labeled cells are closely packed and it is difficult to discriminate between OMP-positive elements. Control and experimental tissues were processed at the same time to minimize differences in OD caused by the experimental procedure. Average gray values in the area of interest were calculated with ImageJ and converted to optical density (OD) by the following formula: OD = log (intensity of background/intensity of area of interest). Mean OD of each olfactory organ was determined for every animal.

Data collected were reported as mean values of each group ± standard error of the mean (SEM) and statistically analyzed by Kruskal–Wallis nonparametric test followed by Mann–Whitney test for multiple comparisons (*P* values adjusted with Holm-Bonferroni correction). *P* values <0.05 were considered significant.

Dual color fluorescence in situ hybridization

Sections of OE from HLA-DQα1-positive mice plus negative control mice from Groups B and C and sections of biopsy specimens of brain and mammary gland were chosen for hybridization with LSI LPL 8p22 SpectrumOrange and LSI C-MYC 8q24.12–24.13 SpectrumGreen human probes (ProVysion, Vysis, ABBOTT Laboratories).

Adjacent slides were incubated with pan-centromeric probes specific to human (labeled with FITC) and mouse (labeled with Cy3) sequences (Cambio) to detect heterokaryons. The slides were dewaxed, dehydrated, digested with Proteinase K/SSC 2X (0.25 mg/mL; Roche Diagnostics) at 45°C for 5 min and postfixed in 4% buffered formalin (Fluka). Sections and probes were then codenatured at 80°C for 10 min for both Vysis and Cambio probes and incubated overnight at 37°C, according to manufacturer's recommendations. They were then stringency washed in 0.3% NP40/SSC 2× at 75°C for 2 min and mounted with DAPI (Kreatech Diagnostics). The prepared slides were observed using an Olympus BX61 epifluorescence microscope system with a JAI CV-M4$^+$ CL digital camera and analyzed with CytoVision 3.7 software.

Electro-olfactograms

Electro-olfactograms (EOGs) were measured by placing glass capillary electrodes at the apical surface of the OE lining the olfactory turbinates and the dorsal region in the sagittally exposed medial olfactory chamber. The test panel of odorants was composed of amyl acetate, cineole, and acetophenone (Sigma), delivered as vapor-phase stimuli (for details, see Pifferi et al. 2009; Franceschini et al. 2009a; Dibattista et al. 2011). The peak amplitude of the EOG response was measured as the maximum negative voltage deflection from baseline. In some mice, the EOG responses were recorded in different points of the same region and data were averaged. Data were reported as average ± SEM, with number of recorded epithelia (n). The statistical significance of data was evaluated as described in Image analysis.

Results

PCR screening

Human xenogenic DNA was detected in PCR amplificates of ADSCs transplanted mice. The presence of the human gene HLA-DQα1 was investigated in the OE, liver, kidney, and skin, at both stages after stem cell inoculation. PCR products obtained from tissues belonging to Groups A and D mice, sacrificed 30 days after transplantation, showed the 242 bp long band corresponding to the amplified human sequence, whereas in negative controls (Groups B and C mice tissues) it was never detected (Figure 2A). However, the intensity of bands from Group D mice sacrificed at the same time was generally very low, and in one case not visible at all (Figure 2B).

Amplificates from mice sacrificed at 60 days after treatment produced very faint bands, or no signal at all (data not shown), probably because the amount of human DNA in the tissues was too low to detect.

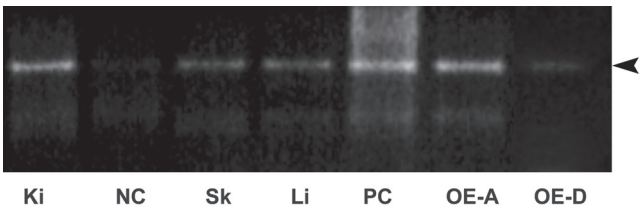

A

Group A 30 days	+	++	++	+	++	+	+	++
Group D	+/-	+/-	-	+/-				

B

Figure 2 PCR reaction and analysis. (**A**) Amplification of HLA-DQα1 gene (242 bp) on 1 mouse from Group A (Ki, Sk, Li, OE-A) and 1 mouse from Group D (OE-D), chosen as representative examples. (**B**) Visual scoring and subjective interpretation of band intensity: (–) no signal, (+/–) barely visible positive signal, (+) moderate positive signal, and (++) intense positive signal. Abbreviations: PC, positive control (DNA from human ADSCs); NC, negative control (DNA from Group C mouse liver); Ki, kidney; Sk, skin; Li, liver; OE-A, olfactory epithelium of Group A mouse; OE-D, olfactory epithelium of Group D mouse.

Lectin staining and immunohistochemistry

DCB effects

As expected, the dorsomedial region of the OE of mice treated with the herbicide was irreversibly damaged. The morphological changes observed in Group B mice were identical to those previously reported (Franceschini et al. 2009a); in brief, the dorsomedial pseudostratified OE was replaced with a thin respiratory-like epithelium, the submucosal tissues appeared fibrotic and most of Bowman's glands and axon bundles had disappeared, with no evidence of regeneration at either 30 or 60 days after the final DCB injection. Morphometric analysis (Figure 3A) revealed a significant decrease in thickness (~75%) compared with the OE of vehicle-treated control mice (Group C) and transplanted non-lesioned mice (Group D), which showed, instead, typical standard morphology.

In addition, the damaged region appeared negative against the pan-neuronal marker PGP 9.5 (Figure 4A), in contrast with the positive staining observed in the lateral undamaged regions and in mice belonging to control groups (Figure 4B,C). However, PCNA-stained cells, mostly close to the basal membrane, were present (Figure 4F). Despite a statistically equivalent rate of proliferation between DCB-treated and non-lesioned mice ($P > 0.05$) (Figure 3B), we observed a significant difference in OMP labeling (Figure 3C): OD values indicated a 4.1-fold decrease compared with DMSO-treated mice, and we could not observe OMP$^+$ mature neurons in the lesioned OE (Figure 4G).

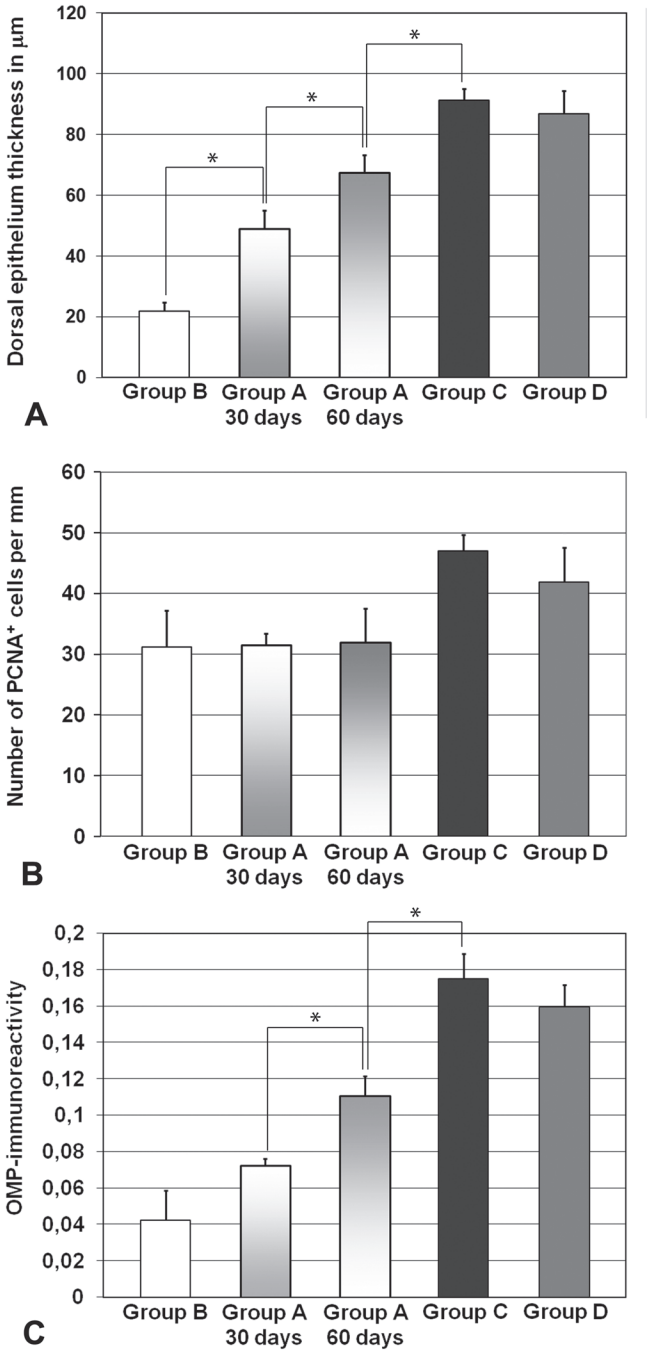

Figure 3 Histological quantitative analysis on dorso-medial OE of all examined groups of mice. In all the graphs, the bars displaying data from Groups B and D refer to tissues sampled at 60 days, but in all control groups there were no significant differences with measurements at 30 days. For this reason, we assumed that Group C not treated mice sacrificed at 30 and 60 days belonged to the same sample group. (**A**) The epithelium is thicker after ADSC transplantation, compared with nontransplanted DCB-treated mice. (**B**) The rate of proliferation appears the same in all groups. (**C**) The amount of mature OSN, indirectly measured through optical density values of OMP immunoreactivity, progressively increases in Group A mice, although it is still lower than in non-lesioned controls. Significant differences are indicated by asterisks: $*P < 0.05$.

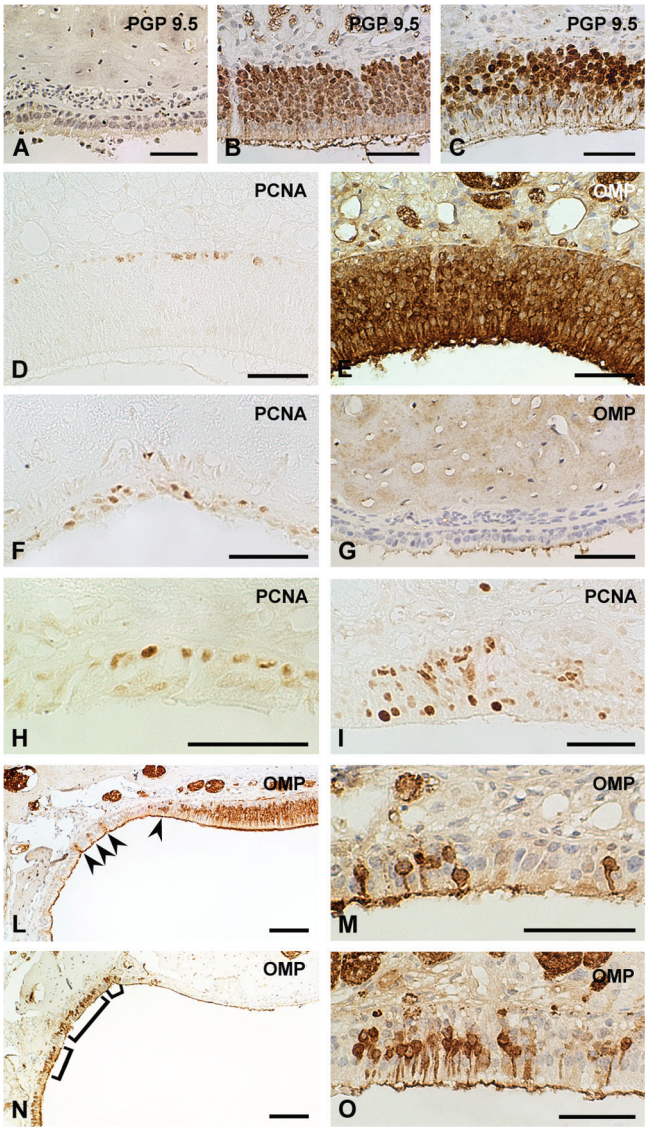

Figure 4 Neuronal population in DCB-sensitive region of Groups B, C, D control mice at 60 days (**A**–**C**). (**A**) PGP 9.5 staining in Group B mice. The OE is substituted by a thin respiratory-like epithelium without PGP 9.5-stained cells. (**B**) PGP 9.5 staining in Group C mice. (**C**) PGP 9.5 staining in Group D mice. Without DCB subministration the morphology of dorsomedial OE is preserved and a great number of PGP 9.5^+ neurons is visible. Comparison of proliferation rate (**D**, **F**, **H**, **I**) and fully differentiated OSNs distribution pattern (**E**, **G**, **L**, **M**, **N**, **O**) in the dorso-medial OE of Groups A, B, C mice. (**D**) PCNA staining in Group C mice. Labeled cells are localized in the basal layer. (**E**) OMP staining in Group C mice. (**F**) PCNA staining in Group B mice. Proliferating cells were distributed in all epithelial layers, as observed also in Group A mice. (**G**) OMP staining in Group B mice. No mature OSNs are present. In the *lamina propria* no olfactory axons and glands are detectable. (**H**) PCNA staining in Group A mice 30 days after DCB subministration. (**I**) PCNA staining in Group A mice 60 days after DCB subministration. (**L**) OMP staining in Group A mice after 30 days at low magnification. Scattered OMP-positive cells are visible (arrows). (**M**) OMP staining in Group A mice 30 days after DCB subministration. Some mature OSN are OMP-positive. Immunoreactive fibers are present in the *lamina propria*. (**N**) OMP staining in Group A mice 60 days after DCB subministration. The number of labeled cells is higher than at 30 days and they are organized in clusters (parentheses). (**O**) OMP staining in Group A mice after 60 days. In the *lamina propria* adenomeres of Bowman's glands are visible. Scale bars = (**A**–**I**, **O**) 50 µm, (**L**, **N**) 100 µm.

ADSCs transplantation

The inoculation of ADSCs stimulated the neuronal recovery in the lesioned olfactory mucosa of Group A mice since we observed a progressive increase in OE thickness (Figure 3A), although it was not uniform along the neuroepithelial length, but limited to some areas of regeneration. Furthermore, we identified new populations of developing OSNs in the dorsomedial neuroepithelium after ADSCs transplantation. At 30 days after treatment, we observed a unicellular layer of BSA-I-B_4^+ elements, characterized by a neuronal pear-shaped soma, lining the basal lamina (Figure 5A). Some cells showed a dendrite-like branch, not yet fully developed, extending towards the apical surface. The identification of scattered groups of more apically located PGP 9.5^+, GAP-43^+, and $TrkB^+$ cells, in the middle region of the OE, just above the germinative layer, confirmed the presence of immature OSNs at various stages of differentiation (Figure 5C,E,G). The GAP-43 and PGP 9.5 reaction products were present not only in the soma but also in the dendrites. Some OMP-stained cells were visible (Figure 4L,M) even if densitometric analysis did not reveal OD levels significantly higher than those registered in Group B mice (Figure 3C).

At 60 days posttransplantation, we could still detect cells differentiating towards neuronal lineage but the OE regeneration appeared incomplete, because both OE depth and OMP-immunoreactive labeling (Figure 3A,C), albeit increased compared with Group A1 mice, were still lower than controls. However, we observed some improvements in neuronal recovery, compared with the previous stage: the clusters of new OSNs that were composed mainly of immunopositive elements, particularly evident in PGP 9.5- (Figure 5D), TrkB- (Figure 5H), and OMP-labeled sections

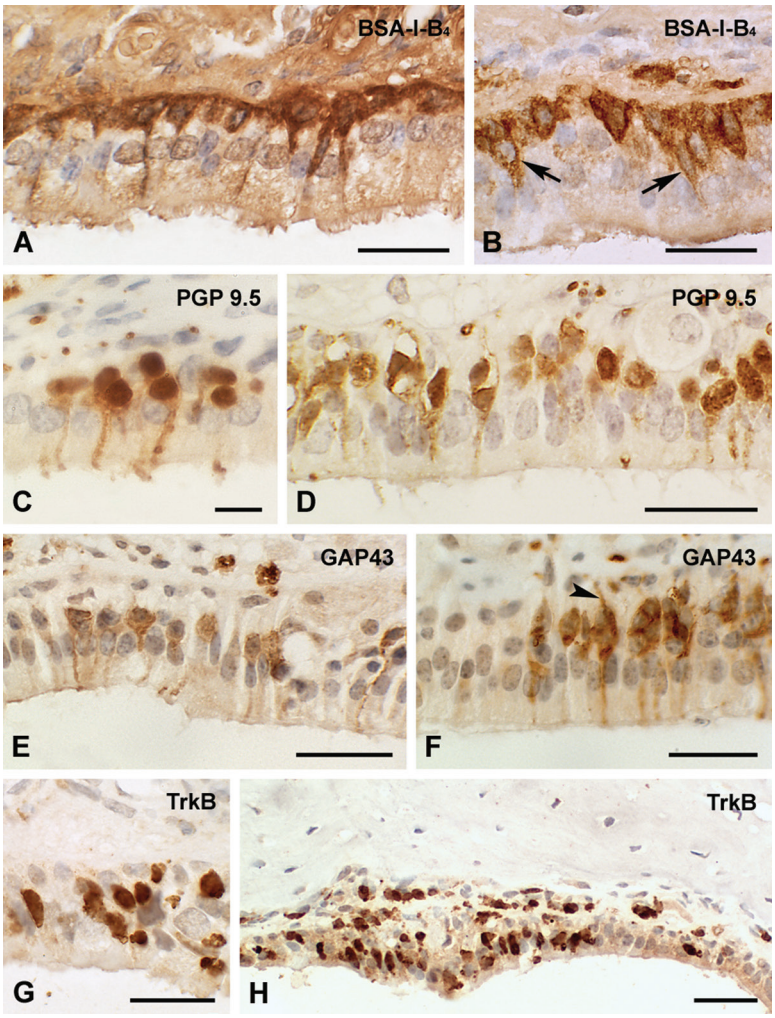

Figure 5 Lectin histochemistry and immunohistochemistry showing neuronal differentiation in dorso-medial OE of Group A mice 30 and 60 days after ADSCs transplantation. A monocellular layer of BSA-I-B_4^+ cells lines the basal lamina at 30 days posttransplantation (**A**), whereas some stained elements are also visible in the second layer after 60 days (arrows) (**B**). At 60 days posttransplantation, the number of PGP 9.5^+ (**D**), GAP-43^+ (**F**), and $TrkB^+$ (**H**) OSNs appears greater than the number of PGP 9.5^+ (**C**), GAP-43^+ (**E**), and $TrkB^+$ (**G**) cells after 30 days, and the epithelium shows a pseudostratified organization 3 to 4 cells thick. Some GAP-43^+ axons are visible near the basal lamina (arrowhead). Scale bars= (**A**, **B**, **D**–**G**) 25 μm, (**C**) 10 μm, (**H**) 50 μm.

(Figure 4N,O), were more extensive. Moreover, GAP-43 staining was visible also in axons emerging from the basal lamina (Figure 5F). Some BSA-I-B_4^+ basal cells also resided in the second layer (Figure 5B).

The responsiveness to stem cell therapy is surprisingly similar in all transplanted mice, because at least some GAP-43-, PGP 9.5-, and OMP positivity were detectable in every animal belonging to Group A. Moreover, the intra-group variability in OMP quantification at 30 and 60 days was low (Figure 3C).

By contrast, the rate of cell proliferation appeared unchanged (Figure 3B) among all treatment groups.

FISH analysis

Some rare nuclei, hybridized with LSI-LPL and LSI C-MYC human probes, were detected in the dorsal region of OE of mice belonging to Group A (Supplementary Figure 1C,D), but none were detected in Groups B and C; in most cases only one of the 2 probe signals was visible, whereas in human tissue they were mostly present in pairs (Supplementary Figure 2B). The presence of human chimeric cells in the olfactory mucosa of treated mice was confirmed by double hybridization with mouse and human centromeric probes (Supplementary Figure 1A,B). In addition, we observed that heterokaryotic nuclei represented the predominant fraction of positive cells. Positive cells were observed in all epithelial layers, basal, middle, and apical. However, some fluorescent signals were also observed in elongated nuclei dispersed in the *lamina propria*, among capillaries and olfactory glia. Positive staining for human DNA was also present in the mucosa underlining the turbinates. Instead heterokaryons were not present in human control tissue (Supplementary Figure 2A).

We found cells with human DNA in specimens from both time stages, despite the negative PCR signal at 60 days.

Electro-olfactograms

EOGs were recorded to evaluate the functional recovery of the OE after ADSCs transplantation in DCB-treated mice. Responses to odorants were recorded both in the dorso-medial region of the OE, damaged by DCB, and in ventral zones that showed no morphological alteration (Figure 6A). We tested amyl acetate, cineole, and acetophenone, which are commonly used odorants and obtained similar results with each one. A representative EOG recording, in response to amyl acetate recorded in the dorsomedial area from a Group C, Group B, and Group A mouse is shown in Figure 6B. The typical odorant response from a control non-treated mouse (left trace) was almost completely abolished in a DCB-treated mouse (middle trace) and recovered in an ADSCs-transplanted mouse (right trace). The average EOG responses in the dorsomedial area, for each mouse group, are plotted in Figure 6C, and demonstrate a significant difference between Groups B and C mice and between Groups

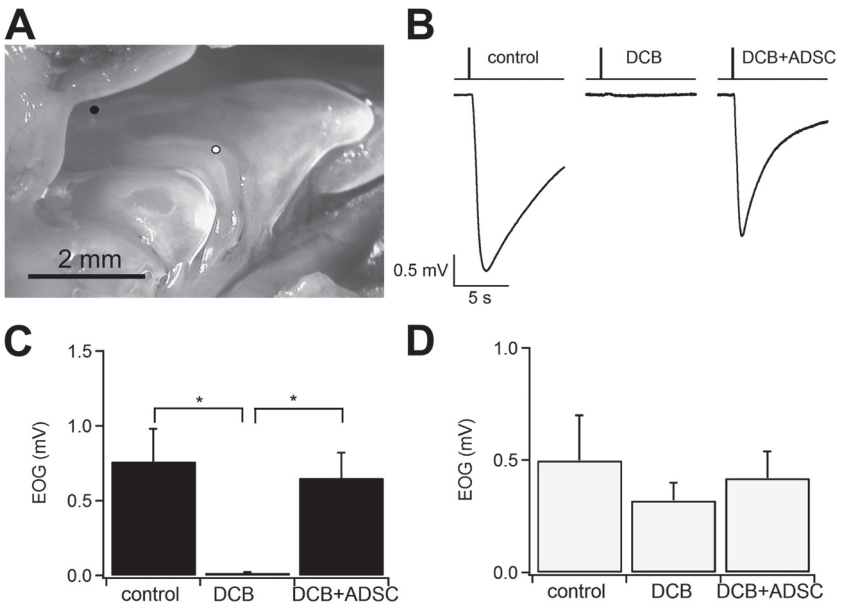

Figure 6 Electro-olfactograms. (**A**) Photomicrograph of exposed mouse olfactory organ. The black spot indicates the DCB-sensitive dorso-medial region, whereas the white spot shows a nonsensitive area in the turbinates. (**B**) Comparison among representative EOGs obtained from recordings in the area indicated by the black spot in (**A**), in response to amyl acetate from a control mouse from Group C, a DCB-treated (DCB) mouse, an ADSCs-transplanted DCB-treated (DCB + ADSCs) mouse after 60 days. The top traces indicate the time of application of the odorant stimulus. (**C**) Average amplitude (±SEM) of EOGs in the sensitive area was significantly different between control and DCB (control: $n = 4$; DCB: $n = 6$) and between DCB+ADSCs and DCB (DCB+ADSCs: $n = 6$). (**D**) Average amplitude of EOGs in the location indicated by the white spot in (**A**) was not significantly different (control: $n = 4$; DCB: $n = 7$; DCB + ADSCs: $n = 6$).

B and A mice. Responses to odorants measured from the area of the OE, indicated by the white spot in Figure 6A, showed no significant difference among the groups of mice ($P > 0.05$; Figure 6D).

Discussion

Our study demonstrated that transplanted ADSCs promoted tissue repair and neuroepithelium regeneration in *nod-scid* mice affected by permanent loss of OSNs in the dorsal OE after treatment with DCB. In contrast, the irreversible toxic effects of this herbicide, associated with the impairment of *lamina propria* and Bowman's glands (Bergman et al. 2002; Franzen et al. 2006), were still visible in nontransplanted mice, in which the dorsal OE remained covered by a ciliated, respiratory-like epithelium after 60 days. We know from literature (Bergman et al. 2002) that just 4 days after the first DCB administration, even at lower doses, OE morphology was totally changed and no differentiating GAP-43$^+$ neurons were present. So, to be sure that the herbicide had completely damaged the dorso-medial olfactory organ before stem cells could engraft and interfere with tissue degeneration, we decided to transplant ADSCs 9 days after the first DCB inoculation.

In all the tissues examined, the engraftment of the stem cells persisted more than 30 days after transplantation, as also reported in our previous study for UCB-CD133$^+$SC (Franceschini et al. 2009a, 2009b). However, it is notable that human ADSCs injected into *nod-scid* recipient mice present an engraftment lifespan of about 60 days (Meyerrose et al. 2007). Accordingly, in tissues sampled on the 60th day we observed a drastic decrease in PCR product yield and in a few cases was barely visible. We also observed quite high intra-group variability in engraftment efficiency owing to different responses to stem cell transplantation from individual recipients, similar to that previously described for human ADSCs retrovirally labeled to express enhanced green fluorescent protein and injected into *nod-scid* mice (Meyerrose et al. 2007). However, the presence of human DNA in DMSO-treated OE appeared less evident (and in 1 sample not detectable) than in Group A mice OE, indicating that transplanted ADSCs are preferentially recruited by damaged tissues. This result is in agreement with the different chimerism values measured by Hess et al. (Hess et al. 2003) in the pancreas of streptozotocin-treated and untreated mice transplanted with bone marrow-derived MSCs. In the central nervous system, it was observed that the percentages of transplanted bone marrow-derived MSCs engrafted in the olfactory bulb of homozygous Purkinje cell degeneration (PCD) mutant mice (Recio et al. 2011) and in the cerebellum of heterozygous PCD mice (Diaz et al. 2012a) were higher than in wild-type mice. Because low doses of i.p.-injected DCB are known to cause tissue-specific toxicity in the olfactory mucosa of rodents with no morphological changes in other tissues (Brandt et al. 1990), the engraftment observed in kidney, liver, and skin could be induced by irradiation (François et al. 2006) rather than a herbicide-mediated damage.

In the dorso-medial OE, regenerative areas, characterized by a significant increase in thickness, were clearly visible and interspersed in the metaplastic epithelium of *nod-scid* mice injected with ADSCs. These regions were colonized by clusters of cells which exhibited pyriform morphology, differentiating dendritic extension and neuronal immunophenotype. We observed also that the proliferative activity appeared unaffected by DCB treatment after 30 days. Mancuso et al. (1997) documented that the rate of cell replication in the *lamina propria* was more sensible to DCB inoculation than in the neuroepithelium, where it barely increased 3 days after toxicant injection. Moreover, even if whole body irradiation seems to stimulate cell division in the Rostral Migratory Stream of adult rats (Bálentová et al. 2006, 2007), we could not observe any effect on proliferation in the OE. BSA-I-B_4 lectin staining, specific for horizontal basal cells (Williams et al. 2004), showed an intact germinative layer, after 30 and 60 days. However, DCB has transient effects on basal cell population because a normal keratin staining pattern (another horizontal basal cell marker) close to the basal lamina was identifiable after 7 weeks (Xie et al. 2013) and 6 months (Bergman et al. 2002) from herbicide i.p. inoculation. Moreover, at a lower dose (30 mg/kg) the restoration of the keratin-positive cell population was completed at 4 weeks posttreatment (Vedin et al. 2004). As a consequence, the permanent effects of DCB seem to be concentrated on the differentiation process, because no immature OSNs could be detected in the DCB-lesioned dorsal OE (Bergman et al. 2002; Vedin et al. 2004; Xie et al. 2013). The presence of PGP 9.5$^+$, TrkB$^+$, GAP-43$^+$, and OMP$^+$ elements, absent in lesioned untransplanted mice, suggested that neurogenesis occurred. Since neurogenesis is necessary, in order to reverse the impairment status, under normal conditions, it is stimulated following damage to the OE and markers for immature neurons are upregulated (Chen et al. 2005). In particular, GAP-43 staining, related to axonal cone growth and glomerular synaptogenesis (Avwenagha et al. 2003), indicates a potential re-establishment of central olfactory nerve connections. Moreover, OMP-immunolabeling confirmed that the process of differentiation reached the last stage with the development of new fully mature OSNs.

In parallel to histological regeneration, functional recovery occurred. Despite a partial histological regeneration of the lesioned dorso-medial OE, the functional recovery appeared completely, because EOG recordings revealed that the olfactory sensitivity, which was almost completely abolished in Group B mice, regained control values in transplanted mice. In the OE of mammals, OR genes have overlapping expression areas, except for the class I OR genes, expressed by OCAM-negative OSNs exclusively localized in the dorso-medial OE (Miyamichi et al. 2005), originally

indicated as "zone I" (Mori et al. 2000; Nagao et al. 2002), from the dorsomedial zone I to the ventrolateral zone IV. High affinity pyridazine and *n*-decyl alcohol receptors are expressed in zone I and the ability to detect these odorants decreased after DCB treatment, whereas receptors for benzene and ethyl acetate, expressed in the ventrolateral-most zones, had no discrepancies in detection threshold (Vedin et al. 2004). In this study, we prepared amyl acetate, cineole, and acetophenone solutions, commonly used in electrophysiological tests, and observed that the significant decline in the odorant response was specific to the dorsomedial region for all 3 chemical substances, whereas no alterations in olfactory capability were recorded in cases in which electrodes were placed in areas other than DCB sensitive ones. We concluded that the receptors for the odorants employed were distributed overall in the olfactory organ with no zone-dependent pattern.

The detection of chimeric cells in the olfactory organ after 30 and 60 days from transplantation confirmed that there was engraftment of human stem cells in the lesioned organ. In addition, the dual color fluorescence in situ hybridization revealed that the proportion of human-mouse hybrid cells was reasonably high. Nuclear reprogramming by cell-to-cell fusion is a possible pathway for stem cell plasticity (Kashofer et al. 2006; Theise 2010), and it is strongly enhanced by dysfunctioning events, as was demonstrated by the high frequency of bone marrow-derived Purkinje heterokaryons in the cerebellum of mice damaged with high-dose irradiation (Wiersema et al. 2007; Espejel et al. 2009) and heterozygous PCD mice (Diaz et al. 2012a). We did not observe polynuclear hybrid cells, therefore we could hypothesize that they underwent hybrid formation followed by reduction division. Such an event displays a high degree of aneuploidy that could lead to unstable heterokaryon formation, with loss of donor genetic material (Duncan et al. 2009) and represents a possible consequence of progressive loss of chromosomes during proliferative cycles. In fact, the majority of heterokaryons, which we identified, did not show LSI-LPL and LSI C-MYC signals together. Unfortunately, it could not be established which chromosomes were lost, as observed also by Kashofer et al. (2006). Moreover, chimeric cells were widely localized in the olfactory organ also, and not only in the OE. Consequently, the phenotype of hybrid cells is variable and hardly predictable. Our data agreed with recent studies, which reported that UCB-CD133^{+}SC or their progeny could fuse with host hepatocytes in *nod-scid*/MPSVII mice with CCl_4-induced liver damage and that the human DNA was gradually eliminated after fusion; even if most human cells were not fused to mouse cells, contrary to our results, fused cells directly improved recovery of the mice from toxic insult (Zhou et al. 2009). Other research has described stem cell fusion as the principal mechanism underlying stem cell therapeutic action (Alvarez-Dolado et al. 2003; Vassilopoulos et al. 2003; Wang et al. 2003; Willenbring et al. 2004; Yoon et al. 2005), and we cannot exclude its potential role in activating the differentiating capability towards neuronal lineage by means of gene expression shift. However, the very low incidence of chimeric cells detected in transplanted mice compared with the amount of OMP- and PGP 9.5-positive cells meant that human stem cells did not represent a significant fraction of the regenerating OE. Perhaps they temporarily remained in the lesioned site, stimulating cell proliferation and differentiation by means of secretion of trophic factors, as previously proposed (Noiseux et al. 2006; Zhou et al. 2009; Sondergaard et al. 2010). During recent years, numerous reports have been published supporting the hypothesis that mesenchymal or bone marrow-derived stem cells promote post-ischemic myocardial repair via paracrine signaling. The factors released may influence adjacent cells and exert their actions via several mechanisms including myocardial protection and neovascularization (Gnecchi et al. 2008; Burdon et al. 2011). Among the broad variety of cytokines, chemokines, and growth factors produced by adult stem cells, some cytoprotective factors, such as vascular endothelial growth factor (VEGF), basic fibroblast growth factor (bFGF), and hepatocyte growth factor (HGF), also showed proangiogenic properties. Moreover, it is known that hematopoietic and mesenchymal stem cells can stimulate activation of cardiac and renal (Tögel et al. 2005) resident stem cells as a consequence of some of their released soluble factors, for example HGF and insulin-like growth factor (IGF)-1 are not only anti-apoptotic but may also enhance proliferation, mobilization, differentiation, and function of endogenous progenitors or even restoration of stem cell niches. More recently, in a murine model of Rett syndrome (Derecki et al. 2012) and PCD mutant mice (Diaz et al. 2012b), microglial cells generated from transplanted bone marrow-derived MSCs reduced neurological disease without neuronal cell replacement: authors proposed that microglia constituted a local source of neuroprotective factors capable of slowing the degenerative process. Similar effects were also recently described for ADSCs, which were discovered to induce nerve repair and growth via BDNF production (Lopatina et al. 2011), and could also explain the massive morphological and functional recovery in the olfactory organ of DCB-treated mice, despite the low number of engrafted stem cells. From this perspective, resident germinative cells, rather than heterokaryons, could be the source of new OSNs in transplanted mice: it has recently been demonstrated that horizontal basal cells can repopulate the DCB-damaged region, even if they generate a metaplastic respiratory epithelium instead of the original OE (Xie et al. 2013). Authors suggested that the cause could be the elimination of some cues that normally drive them to neuro-olfactory differentiation. ADSCs could help to reconstitute the correct environment. However, further studies are necessary to analyze which cell types ADSCs fused with and the fate of heterokaryons in the lesioned tissue.

Conclusions

We demonstrated that ADSCs are actively involved in stimulating recovery from OSNs loss, through migration and engraftment in the damaged area, as well as differentiative induction of new OSNs, contributing to formation of an ideal new microenvironment that stimulates morphogenesis. Stem cell sources may be preferentially chosen by considering the accessibility, abundance, frequency, and expansion potential of the cells. Our findings are encouraging, because they suggest the possibility of a future central role in regenerative medicine for ADSCs, taking into account all their advantages described above. However, as a possible disadvantage, it should be considered that in some patients ADSCs are available to a limited degree (Kern et al. 2006). Moreover, we reported that the histological integrity was only partially restored 60 days after DCB subministration. We cannot exclude that the pool of transplanted stem cells is insufficient for a complete regeneration.

Supplementary material

Supplementary material can be found at http://www.chemse.oxfordjournals.org/

Funding

This work was supported by the Italian Ministry of University and Research (Grant number: FFO10) to V.F., S.B., S.P., and A.M.; Foundation ONLUS "Stem Cells and Life" to V.F. and R.P.R.; and Centre for Clinical Use of Stem Cells (C.U.C.C.S.) to G.S.

Acknowledgements

V.F.: conception and design, data analysis and interpretation, financial support, manuscript wrting; S.B.: collection and assembly of data, data analysis and interpretation, manuscript writing; S.P.: collection and assembly of data, data analysis and interpretation, manuscript writing; A.M.: data analysis and interpretation, manuscript writing; G.S.: financial support; E.O.: provision of study material; A.T.B.: provision of study material; E.D.: data analysis and interpretation; R.P.R.: conception and design, data analysis and interpretation, financial support, manuscript writing.

References

Alvarez-Dolado M, Pardal R, Garcia-Verdugo JM, Fike JR, Lee HO, Pfeffer K, Lois C, Morrison SJ, Alvarez-Buylla A. 2003. Fusion of bone-marrow-derived cells with Purkinje neurons, cardiomyocytes and hepatocytes. Nature. 425(6961):968–973.

Avwenagha O, Campbell G, Bird MM. 2003. Distribution of GAP-43, beta-III tubulin and F-actin in developing and regenerating axons and their growth cones in vitro, following neurotrophin treatment. J Neurocytol. 32(9):1077–1089.

Bálentová S, Raceková E, Martoncíková M, Misúrová E. 2006. Cell proliferation in the adult rat rostral migratory stream following exposure to gamma irradiation. Cell Mol Neurobiol. 26(7–8):1131–1139.

Bálentová S, Raceková E, Misúrová E. 2007. Effect of low-dose irradiation on proliferation dynamics in the rostral migratory stream of adult rats. Folia Biol (Praha). 53(3):74–78.

Bergman U, Ostergren A, Gustafson AL, Brittebo B. 2002. Differential effects of olfactory toxicants on olfactory regeneration. Arch Toxicol. 76(2):104–112.

Bettini S, Ciani F, Franceschini V. 2006. Recovery of the olfactory receptor neurons in the African Tilapia mariae following exposure to low copper level. Aquat Toxicol. 76(3–4):321–328.

Brandt I, Brittebo EB, Feil VJ, Bakke JE. 1990. Irreversible binding and toxicity of the herbicide dichlobenil (2,6-dichlorobenzonitrile) in the olfactory mucosa of mice. Toxicol Appl Pharmacol. 103(3):491–501.

Burdon TJ, Paul A, Noiseux N, Prakash S, Shum-Tim D. 2011. Bone marrow stem cell derived paracrine factors for regenerative medicine: current perspectives and therapeutic potential. Bone Marrow Res. 2011:1–14.

Buron G, Hacquemand R, Pourié G, Brand G. 2009. Inhalation exposure to acetone induces selective damage on olfactory neuroepithelium in mice. Neurotoxicology. 30(1):114–120.

Chen H, Kohno K, Gong Q. 2005. Conditional ablation of mature olfactory sensory neurons mediated by diphtheria toxin receptor. J Neurocytol. 34(1-2):37–47.

Chen J, Tang YX, Liu YM, Chen J, Hu XQ, Liu N, Wang SX, Zhang Y, Zeng WG, Ni HJ, *et al*. 2012. Transplantation of adipose-derived stem cells is associated with neural differentiation and functional improvement in a rat model of intracerebral hemorrhage. CNS Neurosci Ther. 18(10):847–854.

Chi GF, Kim MR, Kim DW, Jiang MH, Son Y. 2010. Schwann cells differentiated from spheroid-forming cells of rat subcutaneous fat tissue myelinate axons in the spinal cord injury. Exp Neurol. 222(2):304–317.

Cruzan G, Carlson GP, Johnson KA, Andrews LS, Banton MI, Bevan C, Cushman JR. 2002. Styrene respiratory tract toxicity and mouse lung tumors are mediated by CYP2F-generated metabolites. Regul Toxicol Pharmacol. 35(3):308–319.

De Girolamo L, Sartori MF, Albisetti W, Brini AT. 2007. Osteogenic differentiation of human adipose-derived stem cells: comparison of two different inductive media. J Tissue Eng Regen Med. 1(2):154–157.

Derecki NC, Cronk JC, Lu Z, Xu E, Abbott SB, Guyenet PG, Kipnis J. 2012. Wild-type microglia arrest pathology in a mouse model of Rett syndrome. Nature. 484(7392):105–109.

Dhar S, Yoon ES, Kachgal S, Evans GR. 2007. Long-term maintenance of neuronally differentiated human adipose tissue-derived stem cells. Tissue Eng. 13(11):2625–2632.

Diaz D, Lepousez G, Gheusi G, Alonso JR, Lledo PM, Weruaga E. 2012. Bone marrow cell transplantation restores olfaction in the degenerated olfactory bulb. J Neurosci. 32(26):9053–9058.

Diaz D, Recio JS, Weruaga E, Alonso JR. 2012. Mild cerebellar neurodegeneration of aged heterozygous PCD mice increases cell fusion of Purkinje and bone marrow-derived cells. Cell Transplant. 21(7):1595–1602.

Dibattista M, Massimino ML, Maurya DK, Menini A, Bertoli A, Sorgato MC. 2011. The cellular prion protein is expressed in olfactory sensory neurons of adult mice but does not affect the early events of the olfactory transduction pathway. Chem Senses. 36(9):791–797.

Duncan AW, Hickey RD, Paulk NK, Culberson AJ, Olson SB, Finegold MJ, Grompe M. 2009. Ploidy reductions in murine fusion-derived hepatocytes. PLoS Genet. 5(2):e1000385.

Espejel S, Romero R, Alvarez-Buylla A. 2009. Radiation damage increases Purkinje neuron heterokaryons in neonatal cerebellum. Ann Neurol. 66(1):100–109.

Farbman AI. 1990. Olfactory neurogenesis: genetic or environmental controls? Trends Neurosci. 13(9):362–365.

Franceschini V, Bettini S, Pifferi S, Rosellini A, Menini A, Saccardi R, Ognio E, Jeffery R, Poulsom R, Revoltella RP. 2009a. Human cord blood CD133+ stem cells transplanted to nod-scid mice provide conditions for regeneration of olfactory neuroepithelium after permanent damage induced by dichlobenil. Stem Cells. 27(4):825–835.

Franceschini V, Bettini S, Saccardi S, Revoltella RP. 2009b. Stem cells transplantation supports the repair of injured olfactory neuroepithelium after permanent lesion. In: Baharvand H, editor. Trends in stem cell biology and technology. Totowa (NJ): Humana Press. p. 283–297.

François S, Bensidhoum M, Mouiseddine M, Mazurier C, Allenet B, Semont A, Frick J, Saché A, Bouchet S, Thierry D, *et al*. 2006. Local irradiation not only induces homing of human mesenchymal stem cells at exposed sites but promotes their widespread engraftment to multiple organs: a study of their quantitative distribution after irradiation damage. Stem Cells. 24(4):1020–1029.

Franzen A, Carlsson C, Hermansson V, Lang M, Brittebo EB. 2006. CYP2A5-mediated activation and early ultrastructural changes in the olfactory mucosa: studies on 2,6-dichlorophenyl methylsulfone. Drug Metab Dispos. 34(1):61–68.

Gnecchi M, Zhang Z, Ni A, Dzau VJ. 2008. Paracrine mechanisms in adult stem cell signaling and therapy. Circ Res. 103(11):1204–1219.

Gögel S, Gubernator M, Minger SL. 2011. Progress and prospects: stem cells and neurological diseases. Gene Ther. 18(1):1–6.

Gu JH, Ji YH, Dhong ES, Kim DH, Yoon ES. 2012. Transplantation of adipose derived stem cells for peripheral nerve regeneration in sciatic nerve defects of the rat. Curr Stem Cell Res Ther. 7(5):347–355.

Hess D, Li L, Martin M, Sakano S, Hill D, Strutt B, Thyssen S, Gray DA, Bhatia M. 2003. Bone marrow-derived stem cells initiate pancreatic regeneration. Nat Biotechnol. 21(7):763–770.

Jacquot L, Pourie G, Buron G, Monnin J, Brand G. 2006. Effects of toluene inhalation exposure on olfactory functioning: behavioral and histological assessment. Toxicol Lett. 165(1):57–65.

Jang S, Cho HH, Cho YB, Park JS, Jeong HS. 2010. Functional neural differentiation of human adipose tissue-derived stem cells using bFGF and forskolin. BMC Cell Biol. 11:25.

Kasai T, Nishizawa T, Arito H, Nagano K, Yamamoto S, Matsushima T, Kawamoto T. 2002. Acute and subchronic inhalation toxicity of chloroform in rats and mice. J Occup Health. 44:193–202.

Kashofer K, Siapati EK, Bonnet D. 2006. In vivo formation of unstable heterokaryons after liver damage and hematopoietic stem cell/progenitor transplantation. Stem Cells. 24(4):1104–1112.

Keller M, Douhard Q, Baum MJ, Bakker J. 2006. Destruction of the main olfactory epithelium reduces female sexual behavior and olfactory investigation in female mice. Chem Senses. 31(4):315–323.

Kern S, Eichler H, Stoeve J, Klüter H, Bieback K. 2006. Comparative analysis of mesenchymal stem cells from bone marrow, umbilical cord blood, or adipose tissue. Stem Cells. 24(5):1294–1301.

Kim SU, de Vellis J. 2009. Stem cell-based cell therapy in neurological diseases: a review. J Neurosci Res. 87(10):2183–2200.

Kim JW, Hong SL, Lee CH, Jeon EH, Choi AR. 2010. Relationship between olfactory function and olfactory neuronal population in C57BL6 mice injected intraperitoneally with 3-methylindole. Otolaryngol Head Neck Surg. 143(6):837–842.

Lee RH, Kim B, Choi I, Kim H, Choi HS, Suh K, Bae YC, Jung JS. 2004. Characterization and expression analysis of mesenchymal stem cells from human bone marrow and adipose tissue. Cell Physiol Biochem. 14(4-6):311–324.

Lewis JL, Dahl AR. 1995. Olfactory mucosa: composition, enzymatic location, and metabolism. In: Doty RL, editor. Handbook of olfaction and gustation. New York (NY): Marcel Dekker. p. 33–35.

Liu GB, Cheng YX, Feng YK, Pang CJ, Li Q, Wang Y, Jia H, Tong XJ. 2011. Adipose-derived stem cells promote peripheral nerve repair. Arch Med Sci. 7(4):592–596.

Lopatina T, Kalinina N, Karagyaur M, Stambolsky D, Rubina K, Revischin A, Pavlova G, Parfyonova Y, Tkachuk V. 2011. Adipose-derived stem cells stimulate regeneration of peripheral nerves: BDNF secreted by these cells promotes nerve healing and axon growth de novo. PLoS One. 6(3):e17899.

Mancuso M, Giovanetti A, Brittebo EB. 1997. Effects of dichlobenil on ultrastructural morphology and cell replication in the mouse olfactory mucosa. Toxicol Pathol. 25(2):186–194.

Meyerrose TE, De Ugarte DA, Hofling AA, Herrbrich PE, Cordonnier TD, Shultz LD, Eagon JC, Wirthlin L, Sands MS, Hedrick MA, *et al*. 2007. In vivo distribution of human adipose-derived mesenchymal stem cells in novel xenotransplantation models. Stem Cells. 25(1):220–227.

Miyamichi K, Serizawa S, Kimura HM, Sakano H. 2005. Continuous and overlapping expression domains of odorant receptor genes in the olfactory epithelium determine the dorsal/ventral positioning of glomeruli in the olfactory bulb. J Neurosci. 25(14):3586–3592.

Monticello TM, Morgan KT, Hurtt ME. 1990. Unit length as the denominator for quantitation of cell proliferation in nasal epithelia. Toxicol Pathol. 18(1 Pt 1):24–31.

Mori I, Goshima F, Imai Y, Kohsaka S, Sugiyama T, Yoshida T, Yokochi T, Nishiyama Y, Kimura Y. 2002. Olfactory receptor neurons prevent dissemination of neurovirulent influenza A virus into the brain by undergoing virus-induced apoptosis. J Gen Virol. 83(Pt 9):2109–2116.

Mori K, von Campenhause H, Yoshihara Y. 2000. Zonal organization of the mammalian main and accessory olfactory systems. Philos Trans R Soc Lond B Biol Sci. 355(1404):1801–1812.

Mori K, Yoshihara Y. 1995. Molecular recognition and olfactory processing in the mammalian olfactory system. Prog Neurobiol. 45(6):585–619.

Mouiseddine M, Francois S, Semont A, Sache A, Allenet B, Mathieu N, Frick J, Thierry D, Chapel A. 2007. Human mesenchymal stem cells home specifically to radiation-injured tissues in a non-obese diabetes/severe combined immunodeficiency mouse model. Brit J Radiol. 80(Spec No 1):S49–S55.

Nagao H, Yamaguchi M, Takahash Y, Mori K. 2002. Grouping and representation of odorant receptors in domains of the olfactory bulb sensory map. Microsc Res Tech. 58(3):168–175.

Noiseux N, Gnecchi M, Lopez-Ilasaca M, Zhang L, Solomon SD, Deb A, Dzau VJ, Pratt RE. 2006. Mesenchymal stem cells overexpressing Akt dramatically repair infarcted myocardium and improve cardiac function despite infrequent cellular fusion or differentiation. Mol Ther. 14(6):840–850.

Pifferi S, Dibattista M, Sagheddu C, Boccaccio A, Al Qteishat A, Ghirardi F, Tirindelli R, Menini A. 2009. Calcium-activated chloride currents in olfactory sensory neurons from mice lacking bestrophin-2. J Physiol. 587(Pt 17):4265–4279.

Recio JS, Álvarez-Dolado M, Diaz D, Baltanás FC, Piquer-Gil M, Alonso JR, Weruaga E. 2011. Bone marrow contributes simultaneously to different neural types in the central nervous system through different mechanisms of plasticity. Cell Transplant. 20(8):1179–1192.

Safford KM, Hicok KC, Safford SD, Halvorsen YD, Wilkison WO, Gimble JM, Rice HE. 2002. Neurogenic differentiation of murine and human adipose-derived stromal cells. Biochem Biophys Res Commun. 294(2):371–379.

Scholz T, Sumarto A, Krichevsky A, Evans GR. 2011. Neuronal differentiation of human adipose tissue-derived stem cells for peripheral nerve regeneration in vivo. Arch Surg. 146(6):666–674.

Schwob JE, Youngentob SL, Mezza RC. 1995. Reconstitution of the rat olfactory epithelium after methyl bromide-induced lesion. J Comp Neurol. 359(1):15–37.

Schwob JE, Youngentob SL, Mezza RC, Iwema CI, Mezza RC. 1999. Reinnervation of the rat olfactory bulb after Methyl Bromide-induced lesion: timing and extent of reinnervation. J Comp Neurol. 412:439–457.

Shipley MT. 1985. Transport of molecules from nose to brain: transneuronal anterograde and retrograde labeling in the rat olfactory system by wheat germ agglutinin-horseradish peroxidase applied to the nasal epithelium. Brain Res Bull. 15(2):129–142.

Sondergaard CS, Hess DA, Maxwell DJ, Weinheimer C, Rosová I, Creer MH, Piwnica-Worms D, Kovacs A, Pedersen L, Nolta JA. 2010. Human cord blood progenitors with high aldehyde dehydrogenase activity improve vascular density in a model of acute myocardial infarction. J Transl Med. 8:24.

Tabatabai G, Frank B, Möhle R, Weller M, Wick W. 2006. Irradiation and hypoxia promote homing of haematopoietic progenitor cells towards gliomas by TGF-β-dependent HIF-Iα-mediated induction of CXCLI2. Brain. 129(9):2426–2435.

Theise ND. 2010. Stem cell plasticity: recapping the decade, mapping the future. Exp Hematol. 38(7):529–539.

Tjälve H, Henriksson J, Tallkvist J, Larsson BS, Lindquist NG. 1996. Uptake of manganese and cadmium from the nasal mucosa into the central nervous system via olfactory pathways in rats. Pharmacol Toxicol. 79(6):347–356.

Tögel F, Hu Z, Weiss K, Isaac J, Lange C, Westenfelder C. 2005. Administered mesenchymal stem cells protect against ischemic acute renal failure through differentiation independent mechanisms. Am J Physiol. 289(1):F31–F42.

Vassilopoulos G, Wang PR, Russell DW. 2003. Transplanted bone marrow regenerates liver by cell fusion. Nature. 422(6934):901–904.

Vedin V, Slotnick B, Berghard A. 2004. Zonal ablation of the olfactory sensory neuroepithelium of the mouse: effects on odorant detection. Eur J Neurosci. 20(7):1858–1864.

Vent J, Bartels S, Haynatzki G, Gentry-Nielsen MJ, Leopold DA, Hallworth R. 2003. The impact of ethanol and tobacco smoke on intranasal epithelium in the rat. Am J Rhinol. 17(4):241–247.

Vent J, Robinson AM, Gentry-Nielsen MJ, Conley DB, Hallworth R, Leopold DA, Kern RC. 2004. Pathology of the olfactory epithelium: smoking and ethanol exposure. Laryngoscope. 114(8):1383–1388.

Wang X, Willenbring H, Akkari Y, Torimaru Y, Foster M, Al-Dhalimy M, Lagasse E, Finegold M, Olson S, Grompe M. 2003. Cell fusion is the principal source of bone-marrow-derived hepatocytes. Nature. 422(6934):897–901.

Weruaga E, Briñón JG, Porteros A, Arévalo R, Aijón J, Alonso JR. 2000. Expression of neuronal nitric oxide synthase/NADPH-diaphorase during olfactory differentiation and regeneration. Eur J Neurosci. 12(4):1177–1193.

Wiersema A, Dijk F, Dontje B, van der Want JJ, de Haan G. 2007. Cerebellar heterokaryon formation increases with age and after irradiation. Stem Cell Res. 1(2):150–154.

Willenbring H, Bailey AS, Foster M, Akkari Y, Dorrell C, Olson S, Finegold M, Fleming WH, Grompe M. 2004. Myelomonocytic cells are sufficient for therapeutic cell fusion in liver. Nat Med. 10(7):744–748.

Williams SK, Gilbey T, Barnett SC. 2004. Immunohistochemical studies of the cellular changes in the peripheral olfactory system after zinc sulfate nasal irrigation. Neurochem Res. 29(5):891–901.

Xie F, Fang C, Schnittke N, Schwob JE, Ding X. 2013. Mechanisms of permanent loss of olfactory receptor neurons induced by the herbicide 2,6-dichlorobenzonitrile: effects on stem cells and noninvolvement of acute induction of the inflammatory cytokine IL-6. Toxicol Appl Pharmacol. 272(3):598–607.

Xu Y, Liu Z, Liu L, Zhao C, Xiong F, Zhou C, Li Y, Shan Y, Peng F, Zhang C. 2008. Neurospheres from rat adipose-derived stem cells could be induced into functional Schwann cell-like cells in vitro. BMC Neurosci. 9:21.

Yoon YS, Wecker A, Heyd L, Park JS, Tkebuchava T, Kusano K, Hanley A, Scadova H, Qin G, Cha DH, *et al*. 2005. Clonally expanded novel multipotent stem cells from human bone marrow regenerate myocardium after myocardial infarction. J Clin Invest. 115(2):326–338.

Zarzo M. 2007. The sense of smell: molecular basis of odorant recognition. Biol Rev Camb Philos Soc. 82(3):455–479.

Zhou P, Hohm S, Olusanya Y, Hess DA, Nolta J. 2009. Human progenitor cells with high aldehyde dehydrogenase activity efficiently engraft into damaged liver in a novel model. Hepatology. 49(6):1992–2000.

Zuk PA, Zhu M, Ashjian P, De Ugarte DA, Huang JI, Mizuno H, Alfonso ZC, Fraser JK, Benhaim P, Hedrick MH. 2002. Human adipose tissue is a source of multipotent stem cells. Mol Biol Cell. 13(12):4279–4295.